

Double-biprism electron interferometry

Ken Harada, Akira Tonomura, Yoshihiko Togawa, Tetsuya Akashi, and Tsuyoshi Matsuda

Citation: [Applied Physics Letters](#) **84**, 3229 (2004); doi: 10.1063/1.1715155

View online: <http://dx.doi.org/10.1063/1.1715155>

View Table of Contents: <http://scitation.aip.org/content/aip/journal/apl/84/17?ver=pdfcov>

Published by the [AIP Publishing](#)

Articles you may be interested in

[Coherent femtosecond low-energy single-electron pulses for time-resolved diffraction and imaging: A numerical study](#)

J. Appl. Phys. **112**, 113109 (2012); 10.1063/1.4768204

[Spatial-chirp compensation in dynamical holograms reconstructed with ultrafast lasers](#)

Appl. Phys. Lett. **94**, 011104 (2009); 10.1063/1.3063047

[Triple-biprism electron interferometry](#)

J. Appl. Phys. **99**, 113502 (2006); 10.1063/1.2198987

[High-resolution observation by double-biprism electron holography](#)

J. Appl. Phys. **96**, 6097 (2004); 10.1063/1.1803105

[Electron holography of field-emitting nanotubes](#)

AIP Conf. Proc. **591**, 572 (2001); 10.1063/1.1426934



Double-biprism electron interferometry

Ken Harada^{a)} and Akira Tonomura

Frontier Research System, The Institute of Physical and Chemical Research, Hatoyama, Saitama 350-0395, Japan and Advanced Research Laboratory, Hitachi, Ltd., Hatoyama, Saitama 350-0395, Japan

Yoshihiko Togawa

Frontier Research System, The Institute of Physical and Chemical Research, Hatoyama, Saitama 350-0395, Japan

Tetsuya Akashi

Hitachi Instruments Service Co., Ltd., 4-28-8 Yotsuya, Shinjuku-ku, Tokyo 160-0004, Japan

Tsuyoshi Matsuda

Frontier Research System, The Institute of Physical and Chemical Research, Hatoyama, Saitama 350-0395, Japan and Musashino Laboratory, Hitachi Science Systems, Ltd., Hachioji, Tokyo 192-0031, Japan

(Received 13 November 2003; accepted 5 March 2004)

Electron holography based on two electron biprisms was developed. The upper biprism was installed just on the image plane of the objective lens, and the lower one was set between the crossover point and image plane of the magnifying lens. This system was able to control two important parameters of the hologram—fringe space and width of interference region— independently. The system enabled us to perform electron holography and interferometry more flexibly. We confirmed the good performance of the system and did preliminary applications using a 1-MV field-emission electron microscope. © 2004 American Institute of Physics.

[DOI: 10.1063/1.1715155]

Electron interferometry has been realized practically after the invention of electron biprism.¹ For better control of two important parameters of the interferogram, fringe spacing s and width of the interference region W , much effort has been expended on developing electron optical system by using not only a single biprism but also double² or triple³ biprisms. However, independent control of the parameters still remains difficult.

On the other hand, electron holography⁴ is ordinarily performed by just installing a single biprism between the objective and magnifying lenses, except for a few studies on multiple-beam holography.^{5,6} The two parameters s and W are also important for holography, because s determines the spatial resolution of a reconstructed image, and W relates to the observable size of the specimen. An ordinary optical setup of electron holography, however, is unable to control the two parameters independently. Therefore, the electron optical system must be modified every time for each experiment, for instance, installing the biprism between the first and second intermediate lenses for high-resolution holography,⁷ whereas switching off the objective lens for observing superconducting vortices.⁸

The present letter introduces a method of holography that uses two biprisms simultaneously to control the two parameters s and W independently. It also discusses preliminary application results obtained by using a 1-MV field-emission electron microscope.⁹

The electron optical system is illustrated in Fig. 1. The filament electrode of the upper biprism is installed just on the image plane of the objective lens and the filament of the lower biprism is set between the crossover point and image

plane of the magnifying lens. All the geometrical parameters for the optical system are indicated in Fig. 1. Fringe spacing s_{obj} and the width of interference region W_{obj} projected on the specimen plane are described by

$$s_{\text{obj}} = \frac{1}{M_l} \frac{1}{M_u} \frac{a_2 D_l \lambda}{2[\alpha_l a_2 (D_l - L_l) + \alpha_u b_2 D_u]}, \quad (1)$$

$$W_{\text{obj}} = \frac{1}{M_l} \frac{1}{M_u} 2\alpha_l L_l - \frac{1}{M_u} d_u, \quad (2)$$

where λ is the wavelength of the electron beam, d_u is the diameter of the upper filament, and α_u and α_l are the deflection angles produced by each filament electrode. Here, M_u and M_l are the respective magnification factors for the specimen by the upper and lower lenses.

As W_{obj} is independent of upper deflection angle α_u , this leads to s_{obj} and W_{obj} being independently controlled. Furthermore, when the lower filament is located on the crossover point of the magnifying lens, (i.e., $D_l - L_l = 0$), s_{obj} also becomes independent of lower deflection angle α_l from Eq. (1). Consequently, both parameters s_{obj} and W_{obj} can be controlled completely. We constructed the optical system, $D_l - L_l = 0$, using the 1-MV electron microscope, but it might be difficult to place the two biprisms in exact real and reciprocal spaces simultaneously in an ordinary electron microscope. This is why we proposed the system in Fig. 1, which makes it possible to construct in a practical machine.

Figure 2 shows examples in which interference on the hologram is flexibly controlled. Sample specimen is magnesium oxide particles. Panels (a) and (b) in Fig. 2 are recorded at different potentials for the upper biprism of $V_{f1} = -20$ and 50 V, respectively, with a fixed potential for the lower biprism of $V_{f2} = 190$ V. Although s_{obj} is controlled by V_{f1} ,

^{a)}Electronic mail: harada@harl.hitachi.co.jp

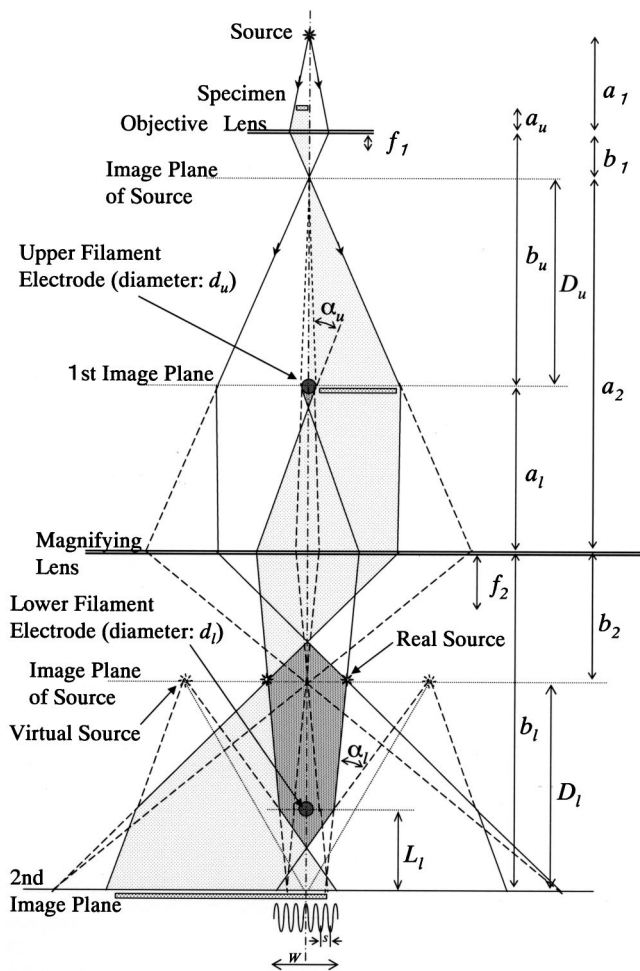


FIG. 1. Schematic diagram of optical system for double-biprism electron holography.

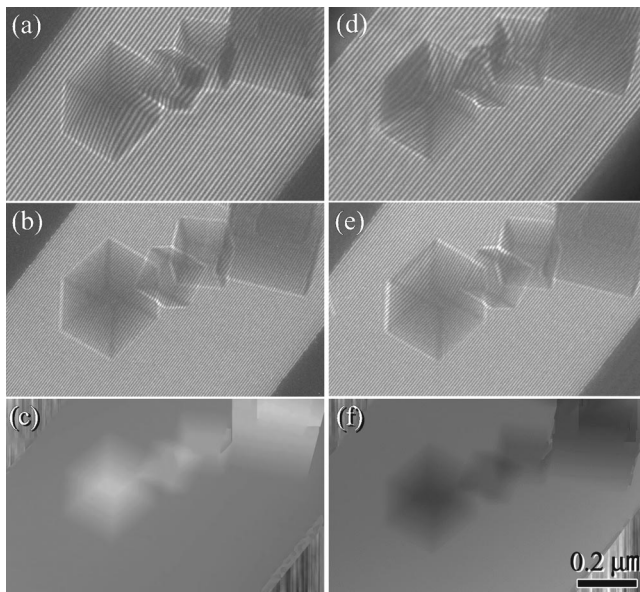


FIG. 2. Electron holograms and their reconstruction phase images: (a) hologram recorded by $V_{f1} = -20$ V and $V_{f2} = 190$ V, (b) by $V_{f1} = 50$ V and $V_{f2} = 190$ V, (c) reconstructed phase images from (b), (d) hologram recorded by $V_{f1} = -200$ V and $V_{f2} = -190$ V, (e) by $V_{f1} = -250$ V and $V_{f2} = -190$ V, (f) reconstructed phase images from (e). The fringe space was controlled by potential V_{f1} on the upper biprism. Both phase shift on the holograms and reconstruction images were reversed in the left and right panels. The entire holograms are free from Fresnel fringes.

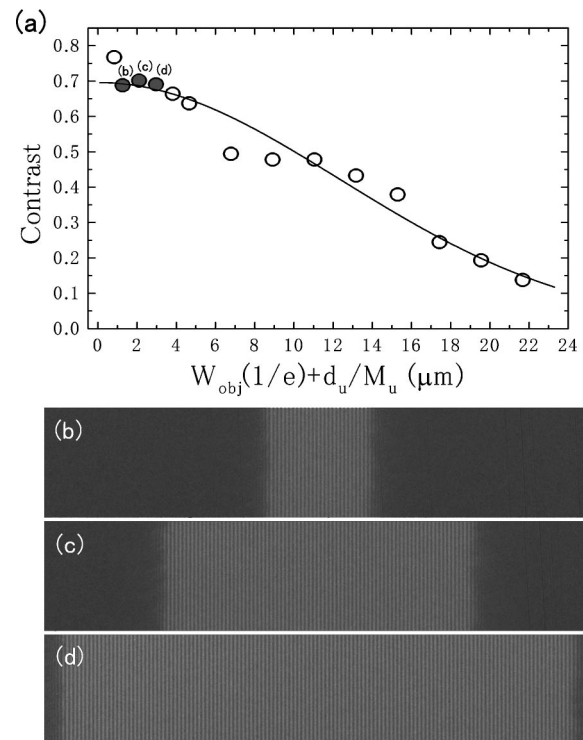


FIG. 3. (a) Fringe contrast versus interference distance as example of coherency measurement of electron beam. Open circles are experimental results and solid line is fitting curve by Gaussian function. Three solid circles highlighted by letters correspond to the micrographs (b), (c), and (d).

W_{obj} did not change. Minimizing of W_{obj} , which is directly related to the spatial coherence of the beam, is an important procedure in order to obtain a high-contrast hologram and a precise phase reconstruction. Panels (d) and (e) are also recorded at different potentials of V_{f1} (-200 and -250 V, respectively), and the potential V_{f2} is negative (-190 V). These two series demonstrate that the present system is able to control the two parameters (s_{obj} and W_{obj}), as well as the angular relation between object and reference waves without the specimen and/or the biprism having to be moved mechanically. This enables easy and precise phase amplification by using the two holograms in the reconstruction process. Panels (c) and (f) are examples of the reconstructed phase images from each series. The reversed contrast of the magnesium oxide particles indicates the reverse angular relation between object and reference waves.

In addition to allowing the interference to be flexibly controlled, the present system has another advantage of *a priori* eliminating of Fresnel fringes.¹⁰ When the lower filament stays inside the shaded area of the upper one, Fresnel fringes are not generated. To satisfy the relation, we chose metal-coated quartz fibers with diameters of 1.6 and 0.8 μm for the upper and lower filaments, respectively.

Being able to independently control s_{obj} and W_{obj} led us to apply the system to measure the spatial coherence¹¹ at the specimen position and to measure the modulation transfer function (MTF) of recording media. The experimental procedures were as follows; spatial coherence was evaluated by fringe contrast, which was achieved by changing the interference distance with fixed s_{obj} . MTF was also evaluated by fringe contrast with changing the spatial frequency of the fringes at a fixed W_{obj} .

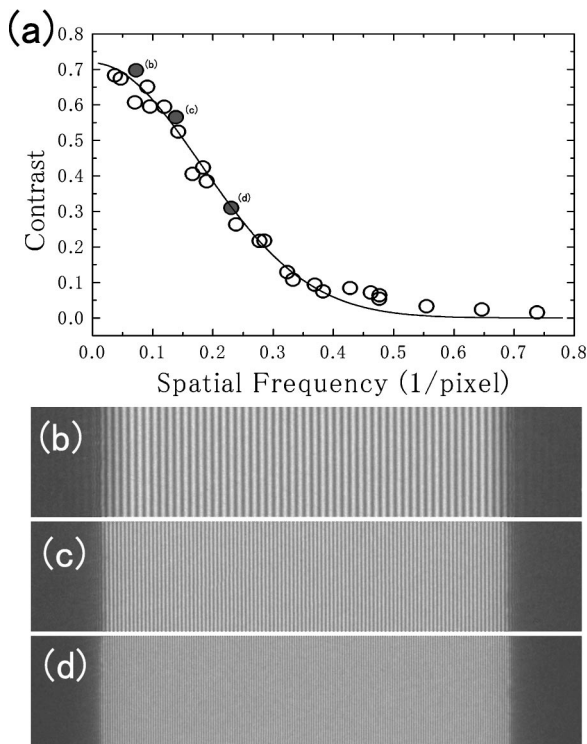


FIG. 4. (a) Fringe contrast versus spatial frequency of interference fringes as example of MTF measurement. Open circles are experimental results and solid line is fitting curve by Gaussian function. Three solid circles highlighted by letters correspond to the micrographs (b), (c), and (d).

Figure 3(a) is an example of coherence function of the 1-MV field-emission electron beam at the specimen position. The illumination condition was for electron holography and the magnification was $10\,000\times$. All the interference fringes were set of 10 pixels/fringe and recorded by a CCD camera of TVIPS F214. The micrographs in Figs. 3(b)–3(d) are examples of observed fringes corresponding to the solid circles. The solid curve in Fig. 3(a), Gaussian function, reveals that we are able to retain an interference fringe with a contrast of 20%, even at about $20\text{-}\mu\text{m}$ distance under the optical condition. From the coherence function, the brightness of electron source B can be calculated with Eq. (3),¹²

$$B = \pi J_0 \left(\frac{W_{\text{obj}}(1/e) + d_u/M_u}{\lambda} \right)^2, \quad (3)$$

where J_0 is a current density on the specimen position and $W_{\text{obj}}(1/e)$ is the width of the interference region when fringe contrast relatively reduced to $1/e$. The calculated brightness

was about $1.6 \times 10^{10} \text{ A/cm}^2 \text{ sr}$ (at $20 \mu\text{A}$ total beam current) which was in good agreement with our previous measurements.^{9,13}

Figure 4(a) is a measured MTF of the CCD camera system under the same optical condition as in the experiment just described. The micrographs in Figs. 4(b)–4(d) are also examples of observed fringes. The MTF in Fig. 4(a) reveals that a low-spatial-frequency signal of 0.1 1/pixel is transferred with high contrast. This is why we chose a fringe spacing of 10 pixels/fringe for the coherence measurement in Fig. 3.

To conclude, we proposed double-biprism electron holography, which enabled us to flexibly control fringe spacing and width of interference region independently. We confirmed its flexibility by recording holograms and doing preliminary application experiments. It should be applied to multi-biprisms if they are available, because the present system does not depend on the number of biprisms. We believe that the system is feasible for advanced electron interferometry, and can be developed for higher applications.

The authors would like to thank Dr. R. E. Dunin-Borkowski of the University of Cambridge and Dr. C. B. Boothroyd of IMRE, Singapore for their support on numerical reconstruction of the holograms. Thanks are also extended N. Moriya of Hitachi Ltd., and Y. Sato, T. Furutsu, I. Matsui, and T. Onai of Hitachi High-Technologies Co. for their technical support.

- ¹G. Möllenstedt and H. Dücker, *Naturwissenschaften* **42**, 41 (1954).
- ²G. Schaal, C. Jönsson, and E. F. Krimmel, *Optik (Stuttgart)* **24**, 529 (1966/1967).
- ³G. Möllenstedt and W. Bayh, *Naturwissenschaften* **49**, 81 (1962).
- ⁴A. Tonomura, *Electron Holography*, 2nd ed. (Springer, Heidelberg, Germany, 1999).
- ⁵T. Kawasaki, G. F. Missiroli, G. Pozzi, and A. Tonomura, *Optik (Stuttgart)* **92**, 168 (1993).
- ⁶T. Hirayama, T. Tanji, and A. Tonomura, *Appl. Phys. Lett.* **67**, 1185 (1995).
- ⁷T. Kawasaki, Q. X. Ru, T. Matsuda, Y. Bando, and A. Tonomura, *Jpn. J. Appl. Phys., Part 2* **30**, L1830 (1991).
- ⁸J. E. Bonevich, K. Harada, T. Matsuda, H. Kasai, T. Yoshida, G. Pozzi, and A. Tonomura, *Phys. Rev. Lett.* **70**, 2952 (1993).
- ⁹T. Kawasaki, T. Yoshida, T. Matsuda, N. Osakabe, A. Tonomura, I. Matsui, and K. Kitazawa, *Appl. Phys. Lett.* **76**, 1342 (2000).
- ¹⁰J. Endo, J. Chen, D. Kobayashi, Y. Wada, and H. Fujita, *Appl. Opt.* **41**, 1308 (2002).
- ¹¹R. Speidel and D. Kurz, *Optik (Stuttgart)* **49**, 173 (1977).
- ¹²G. Pozzi, *Optik (Stuttgart)* **77**, 69 (1987).
- ¹³T. Akashi, K. Harada, T. Matsuda, H. Kasai, A. Tonomura, T. Furutsu, N. Moriya, T. Yoshida, T. Kawasaki, K. Kitazawa, and H. Koinuma, *Appl. Phys. Lett.* **81**, 1922 (2002).